NANO LETTERS

Letter

pubs.acs.org/NanoLett

Low-Dimensional Semiconductor Superlattices Formed by Geometric Control over Nanocrystal Attachment

Wiel H. Evers,[†] Bart Goris,[‡] Sara Bals,[‡] Marianna Casavola,[†] Joost de Graaf,[§] René van Roij,[∥] Marjolein Dijkstra,[§] and Daniël Vanmaekelbergh*[,†]

[†]Condensed Matter and Interfaces, Debye Institute for Nanomaterials Science, Utrecht University, Princetonplein 1, P.O. Box 80.000, 3508 TA, Utrecht, The Netherlands

[‡]EMAT, Department of Physics, University of Antwerpen, Groenenborgerlaan 171, 2010 Antwerpen, Belgium

[§]Soft Condensed Matter, Debye Institute for Nanomaterials Science, Utrecht University, Princetonplein 1, P.O. Box 80.000, 3508 TA, Utrecht, The Netherlands

[∥]Institute for Theorectical Physics, Utrecht University, Leuvenlaan 4, P.O. Box 80.000, 3508 TA, Utrecht, The Netherlands

S *Supporting Information*

ABSTRACT: Oriented attachment, the process in which nanometer-sized crystals fuse by atomic bonding of specific crystal facets, is expected to be more difficult to control than nanocrystal self-assembly that is driven by entropic factors or weak van der Waals attractions. Here, we present a study of oriented attachment of PbSe nanocrystals that counteract this tuition. The reaction was studied in a thin film of the suspension casted on an immiscible liquid at a given temperature. We report that attachment can be controlled such that it occurs with one type of facets exclusively. By control of the temperature and particle concentration we obtain one- or two-dimensional PbSe single crystals, the latter with a honeycomb or square superimposed periodicity in the nanometer range. We demonstrate the ability to convert these PbSe superstructures into other semiconductor compounds with the preservation of crystallinity and geometry.

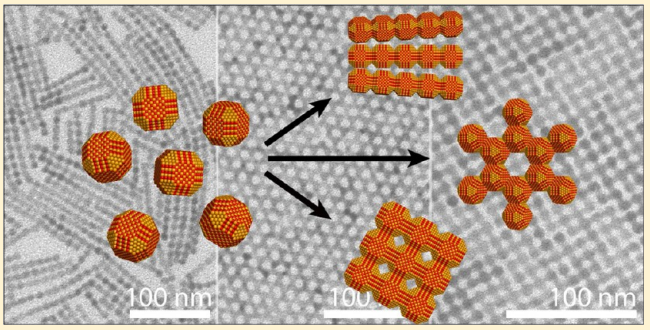

KEYWORDS: *Self-assembly, oriented attachment, nanocrystals, honeycomb, artificial graphene*

Oriented attachment, the connection of a nanometer-sized crystal to another crystal via atomic matching of opposing crystal facets, is an intriguing process that is important in crystal growth and biomineralization.[1−3] In bottom-up approaches that aim to produce extended and highly ordered nanostructures using wet chemistry, oriented attachment is increasingly employed to grow highly anisotropic semiconductor nanostructures.[4−9] This is enabled by recent progress to synthesize colloidal nanocrystals with a uniform size and shape and, hence, with well-defined crystal facets. The adsorption−desorption equilibria of the nanocrystal surfactant molecules, which are responsible for the colloidal stability, are specific for different nanocrystal facets.[10−12] This facet-specific surfactant adsorption can play a decisive role in which facet(s) becomes reactive in nanocrystal attachment, determining in this way the geometry of the resulting structures. In this respect, nanocrystals of the lead chalcogenide family have been studied extensively. By adding specific surfactant molecules or cosolvents to the nanocrystal suspension, specific crystallographic facets can be "activated", resulting in 1-D semiconductor nanowires in some cases and 2-D sheets in other cases. Cho et al. reported the formation of micrometer-long PbSe wires at elevated temperature, formed by the consecutive attachment of PbSe nanocrystals via their opposite {100} facets.[4] More recently, the formation of ultrathin single crystalline PbS sheets initiated by addition of a Cl-containing cosolvent to the suspension was reported.[7] Since the resulting structures are either 1-D wires or 2-D sheets that are highly crystalline, oriented attachment could become a new approach for the fabrication of 1-D and 2-D semiconductors with importance for nanophysics and opto-electronic applications.

Oriented attachment of colloidal nanocrystals is different from nanocrystal self-assembly in the strength of the driving forces, being interatomic bonding in the first and van der Waals interactions or entropic factors in the second case.[13] It can hence be expected that oriented attachment is an irreversible aggregation process that is more difficult to control by the reaction conditions than by nanocrystal self-assembly. Here we present results that counteract this intuition. We studied the oriented attachment of PbSe nanocrystals in a thin film of a suspension casted on an immiscible liquid at temperatures whereby the solvent evaporates. We show that, by variation of

Received: September 6, 2012
Revised: October 8, 2012

   dx.doi.org/10.1021/nl303322k | *Nano Lett.* XXXX, XXX, XXX−XXX

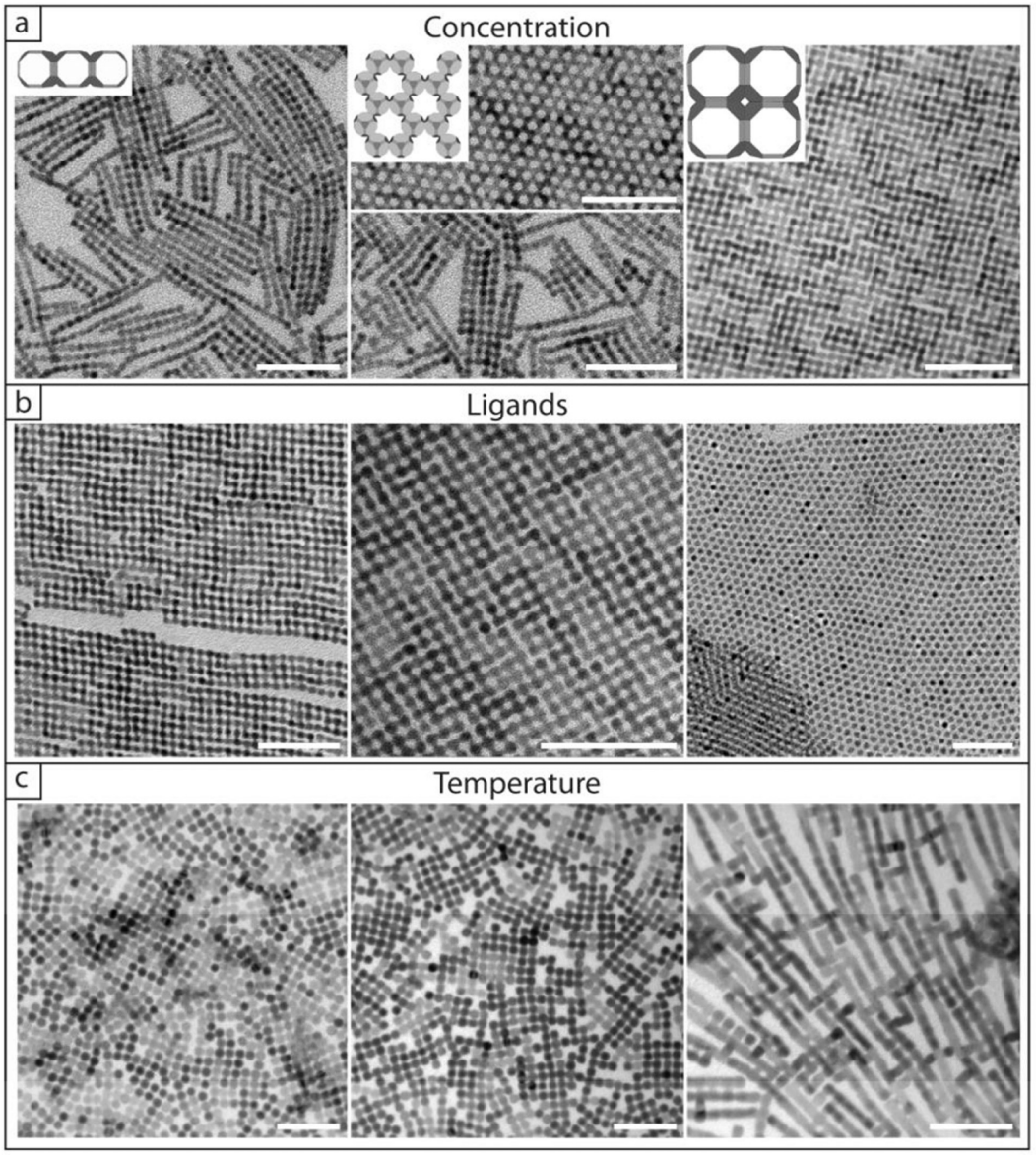

Figure 1. Effects of the reaction parameters on the structures formed by oriented attachment of PbSe nanocrystals. The structural characterization was performed by TEM. (a) Effect of the initial particle concentration in the NC suspension. The colloidal building blocks were truncated PbSe cubes with a size of 5.4 nm capped with oleic acid; the reaction temperature was 50 °C. The initial particle concentrations are: left, 7.0×10^{-7}; center, 11.3×10^{-7}; right, 28×10^{-7} mol/L. No additional capping ligands were added to the ethylene glycol solution. The insets show cartoons of the linear structures, honeycomb superlattices, and ultrathin sheets with square nanostructuring. (b) Effect of oleic acid ligand addition to the ethylene glycol liquid substrate. The building blocks were truncated PbSe cubes with a size of 5.4 nm capped with oleic acid; the reaction temperature was 50 °C, and the initial particle concentration was 28×10^{-7} mol/L. The concentrations of added oleic acid in the ethylene glycol are: left; no additional ligands added, center: 4×10^{-5} mol/L, right: 4×10^{-4} mol/L. (c) Effect of reaction temperature. The building blocks were truncated PbSe cubes with a size of 7.5 nm capped with oleic acid; the initial particle concentration in the suspension was 14×10^{-7} mol/L. The reaction temperature was left: 45, center: 100, and right: 140 °C. All scale bars represent 50 nm. No additional capping ligands were added to the ethylene glycol solution.

the nanocrystal concentration and the temperature, the symmetry of attachment can be varied from linear to two-dimensional and even to three-dimensional. In the two-dimensional case we are able to prepare ultrathin sheets with a square and honeycomb superlattice structure. The resulting structures are suspended on the immiscible substrate liquid and can thus be transferred to any substrate of choice, which enables their incorporation in opto-electronic devices. Moreover, we demonstrate the ability to convert these rods and sheets to other compounds such as CdSe and $Cu_{2-x}Se$, opening the pathway to two-dimensional superlattices of a variety of semiconductor compounds.

We used suspensions of truncated PbSe nanocubes, nanorods, and stars that were nearly uniform in size and shape; high angle annular dark field scanning electron transmission (HAADF-STEM) pictures that present the crystal shapes are given in the Supporting Information (SI). The PbSe nanocubes employed are truncated and appear consistent with a model with 6 {100} initial planes, 12 {110} planes, and 8 {111} planes, and the sizes are varied between 4 and 10 nm. A model is presented in the SI, theoretical section. Typically, 50 μL of

dx.doi.org/10.1021/nl303322k | *Nano Lett.* XXXX, XXX, XXX−XXX

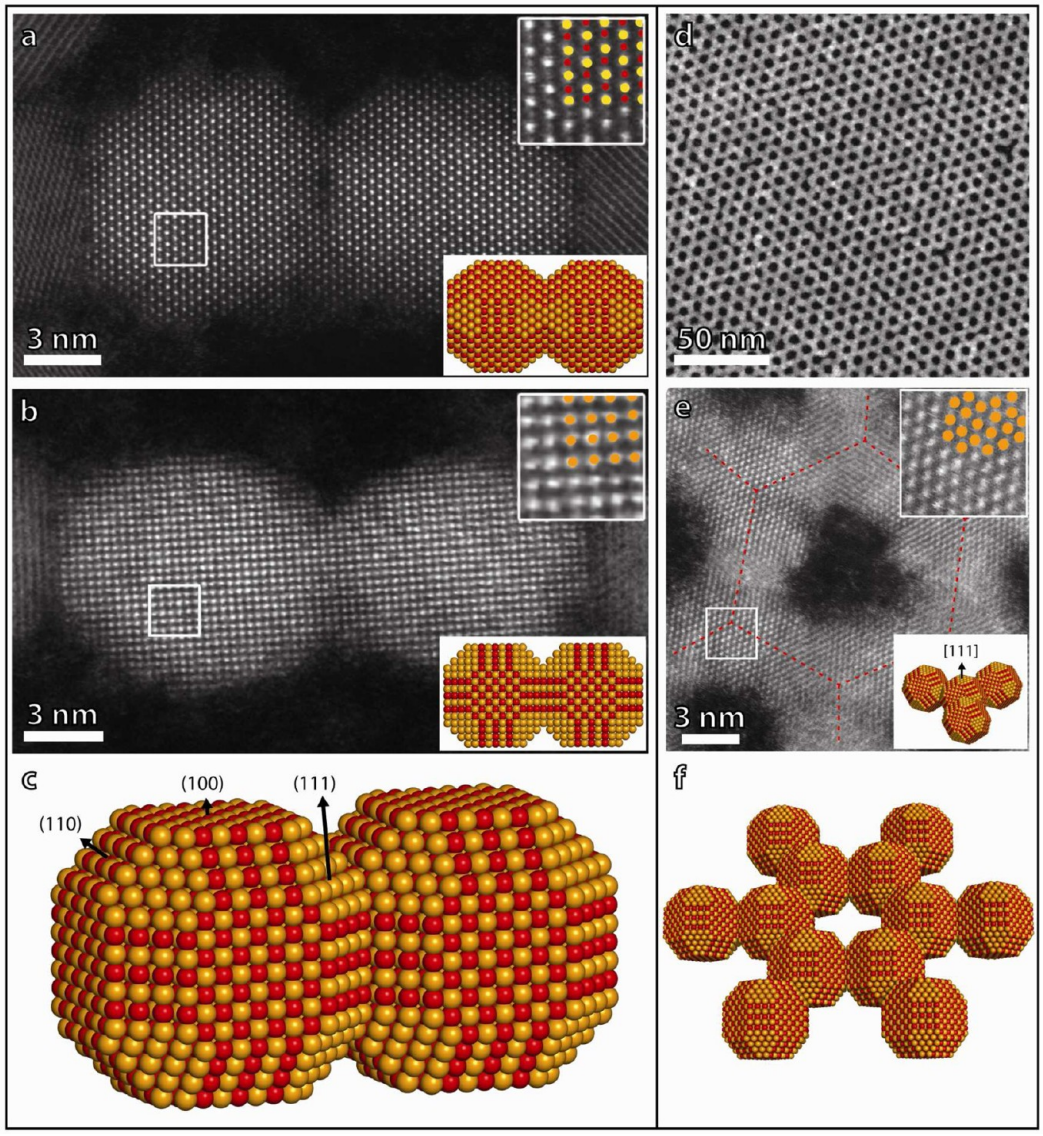

Figure 2. Atomic details of the oriented attachment of PbSe nanocrystals as revealed by HAADF-STEM. Left panel: oriented attachment via {100} facets leading to wires or ultrathin sheets. (a) HAADF-STEM image of two fusing NCs along the [110] projection. (b) HAADF-STEM image of two fusing NCs along the [100] projection. In the inset of a and b, a detailed zoom is given with atomic overlay of the atomic columns (yellow Pb, red Se, orange Pb and Se). The PbSe NCs are attached along the {100}c facets. (c) Model of the two fused NCs. Right panel: Oriented attachment via the {110} facets resulting in a honeycomb superlattice. (d) Overview of the honeycomb lattice; (e) detailed HAADF-STEM picture showing the [111] projection of the original building blocks; (f) 3-dimensional model with atomic resolution showing how the building blocks are attached via the {110} facets.

the suspension was placed on ethylene glycol, being a nearly immiscible liquid for the suspension. The solvent of the suspension was evaporated under a nitrogen atmosphere at a given reaction temperature. The only three parameters that we varied were (i) the initial nanocrystal concentration in the suspension, (ii) the temperature at which the solvent was evaporated, and (iii) the concentration of oleic acid capping molecules that we added into the ethylene glycol substrate liquid. Further details are presented in the SI.

It has been reported that the solvent evaporation in a similar reactor system induces the self-assembly of colloidal nanocrystals into well-ordered and self-supported nanocrystal membranes held together by van der Waals attractions between the capping molecules.[14] In line with this, we observed hexagonally ordered monolayers of PbSe nanocrystals if we used PbSe nanocrystals protected with an inactive CdSe shell (SI, Figure S4A, central panel). However, when we used the oleic acid capped PbSe nanocrystals, the nanocrystal ordering in the structures formed by solvent evaporation changed dramatically and was accompanied by oriented attachment of the crystals, instead of self-assembly driven by van der Waals attractions.

We first review the effect of the three reaction parameters on the structures obtained by nanocrystal attachment; see Figure 1, panels a, b, and c. More complete data sets are presented in the SI, Figures S4−S7. Figure 1 a shows the effect of the initial nanocrystal concentration for nanocrystals of 5.4 nm in size, for a reaction carried out at a temperature of 50 °C. Notice that, at low particle concentrations, the attachment of the nanocrystals led to disordered aggregates; examples are given in the SI (Figure S4). However, above a given nanoparticle concentration, the attachment led to ordered structures with a well-

dx.doi.org/10.1021/nl303322k | *Nano Lett.* XXXX, XXX, XXX−XXX

defined geometry being determined by the nanoparticle concentration. This means that, under given conditions, only one type of facet is active in the crystal bonding, and that there is a directional control in the nanocrystal attachment. The TEM pictures in Figure 1a show that the crystal attachment resulted in nanocrystal wires, a 2-D honeycomb lattice, and finally a 2-D square lattice by simply increasing the particle concentration. Figures S4 and S6 (SI) present the structures formed by 9.9 nm PbSe cubes treated at 100 °C: rod-like systems were observed at $\sim 2 \times 10^{-7}$ mol/L, perfect planar sheets with square nanocrystal ordering at $\sim 11 \times 10^{-7}$ mol/L, and 3-D sheets at particle concentrations larger than $\sim 21 \times 10^{-7}$ mol/L. We remark that the previously reported formation of linear structures or 2-D sheets by attachment of Pb-chalcogenide nanocrystals demands different crystals (PbSe and PbS) and reaction conditions. Here, however, we show that, in one colloidal system, the particle concentration can control the dimensionality and the nanoscale geometry (2-D honeycomb and 2-D square) of the formed structures.

The findings above suggest that the detachment of the capping molecules from specific facets and dissolution of these in the ethylene glycol drives crystal attachment. To further investigate this, we monitored the effect of addition of capping molecules to the ethylene glycol (Figure 1b and SI, Figures S8 and S9). From the results it becomes clear that the addition of sufficient capping molecules to the ethylene glycol stabilizes all facets of the particles, prevents oriented attachment, and leads to the formation of self-assembled hexagonal (mono) layers of stable particles. This shows that the equilibria involving the capping molecules in the suspension (free and attached to the NC facets) and the glycol phase are of primary importance in the controlled reactions that we observe. In this view, the disordered NC aggregation that we observed at low particle concentration can be understood as being the effect of a very low concentration of free ligands in the suspension and the glycol liquid substrate resulting in the stripping of the capping molecules from different NC facets and random crystal attachment.

The effect of the temperature at a given particle concentration can be followed via the horizontal panels of Figure 1C; more examples are presented in the SI, Figures S4, S5, and S7. At a sufficiently high particle concentration, square 2-D sheets formed at lower temperature (45 °C), whereas at higher temperatures (branched) rods were favored.

The results so far showed that the reaction parameters can control the geometry of the formed structures. With the smaller 5.4 nm PbSe particles, there are even two different planar geometries: the honeycomb superlattice and the square sheet. The striking uniformity of the resulting structures shows that only one type of facet is involved in the reaction under given conditions. The atomic details of crystal attachment were further elucidated by a detailed HAADF-STEM[15] study; see Figure 2 and Figures S10–12 and S14 in the SI. Figure 2 a and b shows typical HAADF-STEM images of the linear attachment of two nanocrystals. The atomic columns of Pb and Se can be observed separately along the [110] viewing axis in Figure 2a. Along the [100] viewing axis (Figure 2b), the atomic columns contain both Pb and Se (see atomic overlays). Panel C shows a 3-D illustrative model of how two cubes attached in a linear fashion. For the PbSe wires and square sheets it was observed that crystal attachment occurred mostly via ⟨100⟩/⟨100⟩ connections, while ⟨100⟩/⟨110⟩ and ⟨110⟩/⟨110⟩ connections, breaking the overall square symmetry, are infrequent. Anomalous attachments and defects in the structures can be characterized by HAADF-STEM; see SI, Figure S10. It is clear that, in the example presented in Figure 2a–c, the attachment occurred with full atomic matching of the {100} planes. The connection plane contains columns with considerably less atoms, which is directly related to the shape of the truncated nanocubes involved. The XRD patterns of 2-D sheets formed by oriented attachment indicate that the nanocrystals are uniformly oriented with their [100] axis perpendicular to the substrate, in agreement with attachment involving exclusively the four vertical {100} facets. Further evidence for nearly exclusive attachment via {100} planes followed from the use of PbSe nanorods and stars; see SI, Figures S12–S14. HAADF-STEM showed that the nanorods that we used had a smooth {100} facet termination at both tips, while the long sides are {100} facets that were considerably roughened (SI, Figure S3). In this case, attachment resulted in the formation of wires only, formed by linear connection of the rods without 2-D branching. Possibly, the roughness of the {100} facets at the long sides prevents the formation of 2-D structures. The PbSe stars can be seen as cubes with a pyramid grown on each of the {100} facets. These crystals did not display {100} facets, except for presumably small facets at the tip ends. Strikingly, solvent evaporation at increased temperature led to the formation of attached stars displaying a linear or planar square symmetry; the connections occurred only via the sharp tips. This demonstrates the astounding dominance of the {100} facets in the attachment process. In contrast, however, the remarkable honeycomb superlattices cannot be understood by attachment of the {100} facets. The atomic details of the honeycomb superstructures investigated by HAADF-STEM are presented in Figure 2 d–f. It was observed that the nanocrystals are all oriented with the [111] direction perpendicular to the 2-D sheet plane. Using models for truncated nanocubes, it became clear that this specific orientation is the only way to form a honeycomb lattice and that the {110} facets are exclusively involved in atomic bonding. Three of the 12 {110} facets of each nanocrystal are used, as shown in Figure 2e,f. Theoretical work shows that the {100} facets have a somewhat lower surface energy than the {110} facets and much lower in energy than the {111} facets.[16] This suggest that the dominance of the {100} facets in attachment is due to the fact that at this facet the adsorption equilibrium is shifted the most in the direction of free capping molecules in the suspension and the underlying glycol liquid. The higher energy {110} and Pb-terminated {111} facets remain better protected by the oleic acid capping molecules. That such adsorption/desorption equilibria are key for further understanding is shown by the fact that addition of a small amount of capping molecules in the glycol liquid substrate prevents oriented attachment. However, we should remark that the sudden transition from the linear attachment via {100} facets to the honeycomb lattice via {110} facets to the square sheets again via {100} facets is beyond understanding.

The exclusive use of one type of crystal facets, that is, {100} or {110}, together with the control over the dimensions and the nanoscale geometry by the particle concentration and temperature is remarkable and nontrivial. Here, we attempt to present the main factors that will be required for further understanding. The formation of extended low-dimensional PbSe crystals, that is, wires and square sheets from cubic building blocks that have six equivalent {100} facets, must be the result of symmetry breaking. This indicates that oriented

dx.doi.org/10.1021/nl303322k | Nano Lett. XXXX, XXX, XXX–XXX

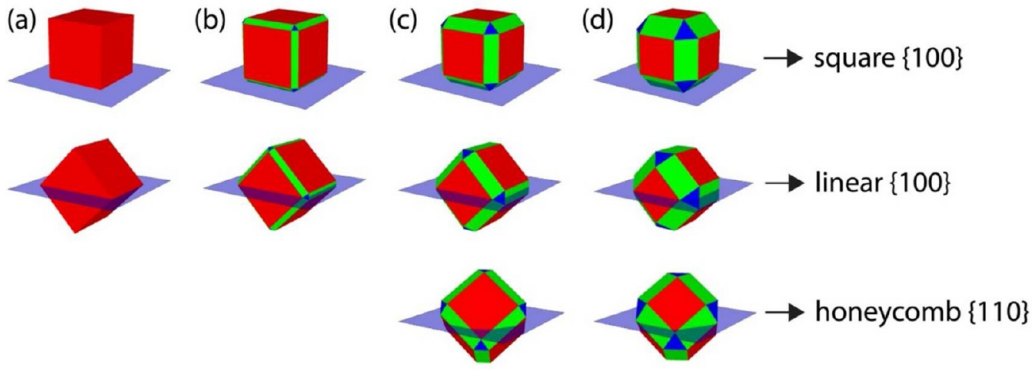

Figure 3. Prototypical equilibrium configurations for truncated PbSe nanocubes adsorbed to a flat toluene−air interface as determined by our theoretical approach; also see the SI section. The level of truncation increases from left to right, and the various crystal facets are indicated using three colors: (red) {100} facets, (green) {110} facets, and (blue) {111} facets. The interface is given by a translucent blue square. (a) For a cube we find exactly two possible adsorption equilibria: one with the normal to one of the {100} facets pointing toward the *z*-axis and one where the normal to one of the {110} "facets" is pointing upward. (b) For slightly greater levels of truncation we again find these two configurations. (c−d) For even greater levels of truncation a third configuration appears, for which the normal to one of the {111} facets is pointing upward.

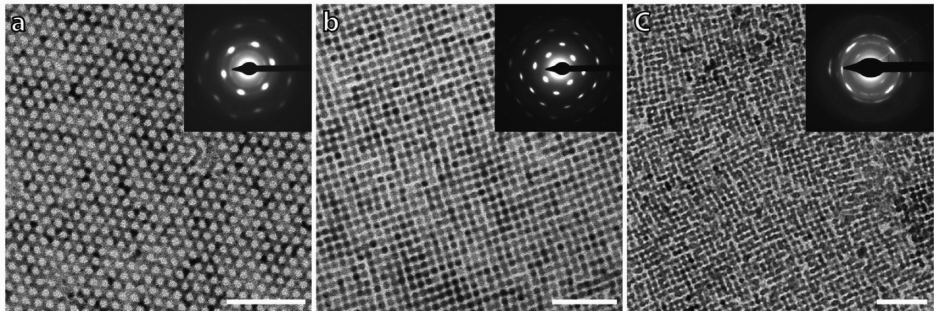

Figure 4. Overview of ultrathin nanostructured semiconductor crystals formed by oriented attachment of 5.4 nm PbSe nanocrystals. (a) Ultrathin PbSe rocksalt semiconductor sheet with a honeycomb nanostructuring. The periodicity of the honeycomb structure is 6.5 nm. Inset: electro-diffractogram showing the PbSe rocksalt lattice in the [111] projection. (b) Ultrathin PbSe rocksalt semiconductor sheet with a square nanostructuring. The periodicity of superlattice structure is 6.6 nm. Inset: electro-diffractogram showing the PbSe rocksalt lattice in the [100] projection. (c) Ultrathin CdSe semiconductor with a compressed zincblende atomic structure and slightly distorted square nanostructuring. Inset: electro-diffractogram showing the CdSe zincblende lattice in the [100] projection. All scale bars represent 50 nm.

attachment in our reactor system takes place at an interface. To support this conjecture, we investigated theoretically the adsorption of our cubic nanocrystals at the air−toluene interface. The experimental system was studied using a simple model of a truncated cube adsorbed at a flat *undeformed* interface, for which only surface-tension contributions to the free energy of adsorption were taken into account. Our model is thus in the spirit of the early investigations of colloid adsorption by Pieranski.[17] We analyzed the equilibrium orientation of the nanocrystals at the interface as a function of the surface properties (as described by the contact angle) of the different types of facet: {100}, {110}, and {111}, which we allowed to vary independently of each other, and as a function of the level of truncation. Remarkably, we found that by varying the contact angles and level of truncation only a limited number of "prototypical" equilibrium adsorption orientations were found. We discuss our findings below and refer to the SI section for further details on the methods used.

We observed that for limited levels of truncation (e.g., for the 9.9 nm PbSe nanocubes) there are two preferred geometries associated to the adsorption, that is, configurations which minimize the free energy. One of the two corresponds to the PbSe nanocube adsorbed at the interface via a {100} facet (Figure 3a,b), while the other one is absorbed via the {110} facet, which implies that respectively the four adjacent or two opposite {100} facets are standing perpendicular to the interface, leaving these free to be involved in oriented attachment in a square- or rod-like fashion in the direction parallel to the plane of the interface, in the way sketched in Figure 2a−c. Alternatively, Cho et al. argued that linear attachment is mediated by a residual electric dipole resulting from the uneven distribution of the {111} Pb and Se facets; once two nanocrystals are attached, the electrical dipole is enhanced leading to further elongation of the rod by new linear attachment events.[4] It should however be remarked that, according to molecular dynamics simulations, the {111} Se planes are considerably reconstructed, leading to a charge reduction.[18] Another point that needs further attention is the formation of the honeycomb superstructures in which each nanocrystal uses three {110} facets. Our calculations show that attachment of the PbSe nanocubes with a [111] direction perpendicular to the interface is one of the three possible adsorption configurations (see Figure 3c,d and SI, theoretical section) that minimize the free energy in case the nanocrystals are considerably truncated (as the 5.4 nm nanocubes). In this adsorption configuration, the truncated {110} planes have an angle of 0.6π with the interface and are available for oriented attachment in the way sketched in Figure 2e,f, resulting in the honeycomb superstructure. It is, however, not easy to understand why the adsorption geometry changes from

dx.doi.org/10.1021/nl303322k | *Nano Lett.* XXXX, XXX, XXX−XXX

perpendicular [111] to [100] by simply increasing the particle concentration.

The two-step bottom-up method that we present here, that is, the synthesis of well-defined nanocrystals from atomic precursors, followed by oriented attachment under mild conditions in a thin film of suspension casted on an immiscible liquid, holds promise for the fabrication of one and two-dimensional semiconductors with applications in nanophysics and opto-electronic devices.[14,19,20] The work presented above shows that, with PbSe nanocube building blocks, simple reaction parameters such as the temperature and particle concentration can be used to prepare 1-D rods and 2-D nanostructured sheets at will. Moreover, the reaction can be moderated by controlled addition of oleic acid capping molecules to the ethylene glycol substrate. The use of a liquid ethylene glycol substrate has another important asset: the products of oriented attachment are suspended on a liquid substrate and can, in this way, be transferred to a solid substrate or an electrical device or be used in soft printing techniques. Some examples of two-dimensional ultrathin sheets with a honeycomb and square nanostructuring are presented in Figure 4. The electro-diffractograms presented in the insets of Figure 4 a,b show that overall the structures are single crystalline (rocksalt PbSe) with an added superstructure periodicity in the nanometer range. This is in line with HAADF-STEM results displayed in Figure 2 that show smooth atomic connections between the nanocrystals. Recently, there has been much interest in the effects of superperiodicity on the electronic properties of semiconductors and confined two-dimensional electron gases.[21−24] It has, for instance, been shown that, when a two-dimensional fermion gas is subject to a honeycomb periodic potential, this results in the emergence of an electronic sub-band with a linear energy-wave vector relationship, in a similar way as for graphene. A honeycomb nanometer periodicity opens thus the possibility to engineer Dirac fermions in various semiconductor compounds. Tight-binding calculations are under way to reveal the electronic sub-bands of the two-dimensional PbSe sheets with a square and honeycomb structure as shown in Figure 4.

While we demonstrated geometric control with nanocrystals of the lead−chalcogenide family, we should remark that the formed one- and two-dimensional semiconductors can be further transformed to other semiconductor compounds by means of cation exchange, while the overall geometry and crystallinity is preserved. For instance, in Figure 4c we showed that the ultrathin PbSe rocksalt sheets can be converted into CdSe zinc blende sheets with preservation of the square nanostructuring. In the SI, Figure S16, we show the conversion of the CdSe sheets to $Cu_{2-x}Se$ sheets. The latter compound opens the gate to use cation exchange to obtain low-dimensional superlattices of various semiconductor compounds.[25−28] Hence, we showed that the low-dimensional PbSe structures prepared by oriented attachment can be transformed to many other compounds while the overall superlattice geometry is preserved. Although many 2-D semiconductors can also be prepared by precious gas-phase methods, the latter methods often do not allow to obtain a superlattice structure with periodicity in the nanometer region, such as the ones we present in Figure 4.

In summary, we have presented results that show that the process of oriented attachment of PbSe nanocrystals can be controlled by simple reaction parameters, resulting in single-crystalline PbSe nanostructures with dimensions between 1 and 3. The ultrathin 2-D sheets are single crystalline and show a super periodicity with planar square or honeycomb geometry. The structures can be picked up on a substrate of choice and can even be transformed to other semiconductor compounds preserving the overall geometry.

■ ASSOCIATED CONTENT

Supporting Information

Additional experimental results and methods are available, including synthesis, characterization of the shapes, oriented attachment of PbSe rods and stars, study of defects and conversion of PbSe sheets to CdSe or $Cu_{2-x}Se$ sheets by ion exchange. Additionally, a theoretical study of the adsorption of PbSe cubes on a liquid−air interface is given. This material is available free of charge via the Internet at http://pubs.acs.org.

■ AUTHOR INFORMATION

Corresponding Author

*E-mail: d.vanmaekelbergh@uu.nl.

Notes

The authors declare no competing financial interest.

■ ACKNOWLEDGMENTS

We wish to acknowledge C. B. Murray for useful discussions. We also wish to acknowledge J. D. Meeldijk for the TEM-EDX measurements. W.H.E., M.C., and D.V. wish to acknowledge NWO-CW for financial support (Topgrant 700.53.308 and Vidi Grant No. 700.56.423). D.V. also acknowledges the Dutch FOM (FP/AV-09.0224) and the European Union under the Seventh Framework Program for financial support (ITN Herodot). S.B. and B.G. are grateful to the Fund for Scientific Research—Flanders and acknowledge financial support from the European Union under the Seventh Framework Program (Integrated Infrastructure Initiative No. 262348 European Soft Matter Infrastructure, ESMI). The authors also acknowledge financial support from the Flemish Hercules 3 programme for large infrastructure. M.D. acknowledges financial support by a NWO Vici Grant and R.v.R. by the Utrecht University High Potential Programme.

■ REFERENCES

(1) Banfield, J. F.; Welch, S. A.; Zhang, H. Z.; Ebert, T. T.; Penn, R. L. *Science* **2000**, *289* (5480), 751−754.
(2) Niederberger, M.; Colfen, H. *Phys. Chem. Chem. Phys.* **2006**, *8* (28), 3271−3287.
(3) Zheng, H.; Smith, R. K.; Jun, Y.-w.; Kisielowski, C.; Dahmen, U.; Alivisatos, A. P. *Science* **2009**, *324* (5932), 1309.
(4) Cho, K. S.; Talapin, D. V.; Gaschler, W.; Murray, C. B. *J. Am. Chem. Soc.* **2005**, *127* (19), 7140−7147.
(5) Yu, Z.; Liu, B.; Ye, B.; Kong, W.; Weng, J.; Wang, Z.; Wang, H. *Rare Metal Mater. Eng.* **2010**, *39*, 133−137.
(6) Pacholski, C.; Kornowski, A.; Weller, H. *Angew. Chem., Int. Ed.* **2002**, *41* (7), 1188.
(7) Schliehe, C.; Juarez, B. H.; Pelletier, M.; Jander, S.; Greshnykh, D.; Nagel, M.; Meyer, A.; Foerster, S.; Kornowski, A.; Klinke, C.; Weller, H. *Science* **2010**, *329* (5991), 550−553.
(8) Xu, F.; Ma, X.; Gerlein, L. F.; Cloutier, S. G. *Nanotechnology* **2011**, *22* (26), 265604.
(9) Koh, W. K.; Bartnik, A. C.; Wise, F. W.; Murray, C. B. *J. Am. Chem. Soc.* **2010**, *132* (11), 3909−3913.
(10) Manna, L.; Milliron, D. J.; Meisel, A.; Scher, E. C.; Alivisatos, A. P. *Nat. Mater.* **2003**, *2* (6), 382−385.
(11) Yin, Y.; Alivisatos, A. P. *Nature* **2005**, *437* (7059), 664−670.
(12) Zhang, J.; Huang, F.; Lin, Z. *Nanoscale* **2010**, *2* (1), 18−34.

(13) Evers, W. H.; De Nijs, B.; Filion, L.; Castillo, S.; Dijkstra, M.; Vanmaekelbergh, D. *Nano Lett.* **2010**, *10* (10), 4235−4241.
(14) Dong, A. G.; Chen, J.; Vora, P. M.; Kikkawa, J. M.; Murray, C. B. *Nature* **2010**, *466* (7305), 474−477.
(15) Bals, S.; Casavola, M.; van Huis, M. A.; Van Aert, S.; Batenburg, K. J.; Van Tendeloo, G.; Vanmaekelbergh, D. *Nano Lett.* **2011**, *11* (8), 3420−3424.
(16) Fang, C. M.; van Huis, M. A.; Vanmaekelbergh, D.; Zandbergen, H. W. *ACS Nano* **2010**, *4* (1), 211−218.
(17) Pieranski, P. *Phys. Rev. Lett.* **1980**, *45* (7), 569−572.
(18) Schapotschnikow, P.; van Huis, M. A.; Zandbergen, H. W.; Vanmaekelbergh, D.; Vlugt, T. J. H. *Nano Lett.* **2010**, *10* (10), 3966−3971.
(19) Talapin, D. V.; Black, C. T.; Kagan, C. R.; Shevchenko, E. V.; Afzali, A.; Murray, C. B. *J. Phys. Chem. C* **2007**, *111* (35), 13244−13249.
(20) Talapin, D. V.; Murray, C. B. *Science* **2005**, *310* (5745), 86−89.
(21) Akhmerov, A. R.; Beenakker, C. W. J. *Phys. Rev. B* **2008**, *77* (8), 085423−085433.
(22) Park, C.-H.; Yang, L.; Son, Y.-W.; Cohen, M. L.; Louie, S. G. *Phys. Rev. Lett.* **2008**, *101* (12), 126804.
(23) Park, C.-H.; Louie, S. G. *Nano Lett.* **2009**, *9* (5), 1793−1797.
(24) Gomes, K. K.; Mar, W.; Ko, W.; Guinea, F.; Manoharan, H. C. *Nature* **2012**, *483* (7389), 306−310.
(25) Li, H.; Brescia, R.; Krahne, R.; Bertoni, G.; Alcocer, M. J. P.; D'Andrea, C.; Scotognella, F.; Tassone, F.; Zanella, M.; De Giorgi, M.; Manna, L. *ACS Nano* **2012**, *6* (2), 1637−1647.
(26) Jain, P. K.; Amirav, L.; Aloni, S.; Alivisatos, A. P. *J. Am. Chem. Soc.* **2010**, *132* (29), 9997−9999.
(27) Li, H.; Zanella, M.; Genovese, A.; Povia, M.; Falqui, A.; Giannini, C.; Manna, L. *Nano Lett.* **2011**, *11* (11), 4964−4970.
(28) Jain, P. K.; Beberwyck, B. J.; Fong, L.-K.; Polking, M. J.; Alivisatos, A. P. *Angew. Chem., Int. Ed.* **2012**, *51* (10), 2387−2390.

dx.doi.org/10.1021/nl303322k | *Nano Lett.* XXXX, XXX, XXX−XXX